Single-Ion Heat Engine at Maximum Power

O. Abah,[1] J. Roßnagel,[2] G. Jacob,[2] S. Deffner,[1,3] F. Schmidt-Kaler,[2] K. Singer,[2] and E. Lutz[1,4]

[1]*Department of Physics, University of Augsburg, D-86159 Augsburg, Germany*
[2]*Quantum, Institut für Physik, Universität Mainz, 55128 Mainz, Germany*
[3]*Department of Chemistry and Biochemistry and Institute for Physical Science and Technology, University of Maryland, College Park, Maryland 20742, USA*
[4]*Dahlem Center for Complex Quantum Systems, Freie Universität Berlin, D-14195 Berlin, Germany*

(Received 17 May 2012; published 14 November 2012)

We propose an experimental scheme to realize a nanoheat engine with a single ion. An Otto cycle may be implemented by confining the ion in a linear Paul trap with tapered geometry and coupling it to engineered laser reservoirs. The quantum efficiency at maximum power is analytically determined in various regimes. Moreover, Monte Carlo simulations of the engine are performed that demonstrate its feasibility and its ability to operate at a maximum efficiency of 30% under realistic conditions.

DOI: 10.1103/PhysRevLett.109.203006 PACS numbers: 37.10.Ty, 05.70.−a, 37.10.Vz

Miniaturization has lead to the development of increasingly smaller devices. This ongoing size reduction from the macroscale to the nanoscale is approaching the ultimate limit, given by the atomic nature of matter [1]. Prominent macrodevices are heat engines that convert thermal energy into mechanical work, and hence motion [2]. A fundamental question is whether these machines can be scaled down to the single particle level, while retaining the same working principles as, for instance, those of a car engine. It is interesting to note in this context that biological molecular motors are based on completely different mechanisms that exploit the constructive role of thermal fluctuations [3,4]. At the nanoscale, quantum properties become important and have thus to be fully taken into account. Quantum heat engines have been the subject of extensive theoretical studies in the last fifty years [5–14]. However, while classical micro heat engines have been fabricated, using optomechanical [15], micro-electromechanical [16–18], and colloidal systems [19], to date no quantum heat engine has been built.

In this Letter, we take a step towards that goal by proposing a single ion heat engine using a linear Paul trap. Specifically, we present a scheme which has the potential to implement a quantum Otto cycle using currently available state-of-the-art ion-trap technology. Laser-cooled ions in linear Paul traps are quantum systems with remarkable properties [20]: they offer an unprecedented degree of preparation and control of their parameters, permit their cooling to the ground state, and allow the coupling to engineered reservoirs [21]. For these reasons, they have played a prominent role in the experimental study of quantum computation and information processing applications [22,23]. They are also invaluable tools for the investigation of quantum thermodynamics [24]. The quantum Otto cycle for a harmonic oscillator is a quantum generalization of the common four-stroke car engine and a paradigm for thermodynamic quantum devices [25–27]. It consists of two isentropic processes during which the frequency of the oscillator (the trap frequency) is varied, and of two isochoric processes, that correspond to a change of temperature at constant frequency, see Fig. 1(a). In the present proposal, we simulate the Otto cycle by confining a single ion in a novel trap geometry with an asymmetric electrode configuration [see Fig. 1(c)] and coupling it alternatingly to two engineered laser reservoirs. As for all realistic machines, this Otto engine runs in finite time and has thus

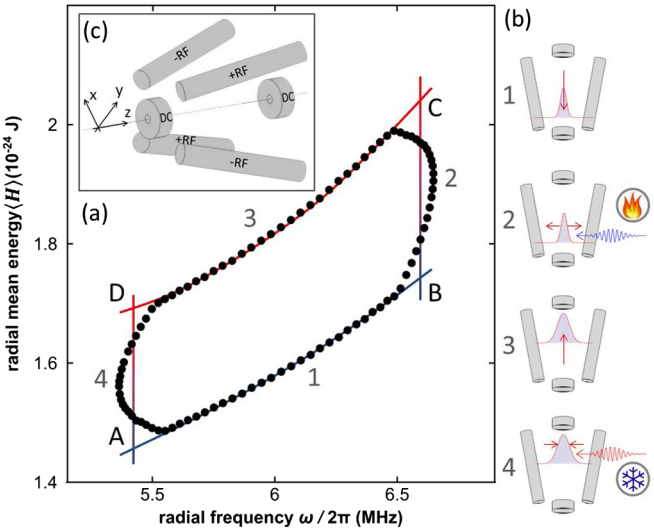

FIG. 1 (color online). (a) Energy-frequency diagram of the Otto cycle for the radial mode of the ion. The continuous line represents the ideal process, while the dots show the results of the Monte Carlo simulations. (b) The pictograms illustrate the four individual strokes of the cycle for the radial state. (c) Geometry of the tapered Paul trap: the rf electrodes have an angle of $\theta = 20°$ with the trap axis, the length of the trap is 5 mm, the radial distance of the ion to the rf electrodes is $r_0 = 1$ mm. The axial and radial frequencies of the trap are $\omega_{0,z}/(2\pi) \simeq 6$ MHz and $\omega_{0,x}/(2\pi) = \omega_{0,y}/(2\pi) \simeq 35$ kHz.

nonzero power [28]. We determine the efficiency at maximum power in the limit of adiabatic and strongly nonadiabatic processes, which we express in terms of the nonadiabaticity parameter introduced by Husimi [29]. We further present semiclassical Monte Carlo simulations, with realistic parameters, that demonstrate the experimental feasibility of such a device. The single ion trap design idea has several advantages. First, all of the parameters of the engine, in particular the bath temperatures, are tunable over a wide range. As a result, maximum power can be achieved. Moreover, at low temperatures, the engine may operate in the quantum regime, where the discreteness of the energy spectrum plays an important role. In addition, the coupling to the laser reservoirs can be either switched on and off externally, or by the intrinsic dynamics of the ion itself. In the latter, the engine runs autonomously [30]. Finally, we introduce a generic mechanism to store the energy produced [7]. Since trapped ions are perfect oscillator models, the results described here may be extended to analogous systems, such as micro- and nanomechanical oscillators [31–34], offering a broad spectrum of potential applications.

Quantum Otto cycle.—We consider a quantum engine whose working medium is a single harmonic oscillator with time-dependent frequency ω_t, changing between ω_1 and ω_2. The engine is alternatingly coupled to two heat baths at inverse temperatures $\beta_i = 1/(k_B T_i)$ $(i = 1, 2)$, where k_B is the Boltzmann constant. The Otto cycle consists of four consecutive steps as shown in Fig. 1(a). (1) *Isentropic compression* $A(\omega_1, \beta_1) \rightarrow B(\omega_2, \beta_1)$: the frequency is varied during time τ_1 while the system is isolated. The evolution is unitary and the von Neumann entropy of the oscillator is thus constant. Note that state B is nonthermal even for slow (adiabatic) processes. (2) *Hot isochore* $B(\omega_2, \beta_1) \rightarrow C(\omega_2, \beta_2)$: the oscillator is weakly coupled to a reservoir at inverse temperature β_2 at fixed frequency and allowed to relax during time τ_2 to the thermal state C. This equilibration is much shorter than the expansion or compression phases (see below). (3) *Isentropic expansion* $C(\omega_2, \beta_2) \rightarrow D(\omega_1, \beta_2)$: the frequency is changed back to its initial value during time τ_3. The isolated oscillator evolves unitarily into the nonthermal state D at constant entropy. (4) *Cold isochore* $D(\omega_1, \beta_2) \rightarrow A(\omega_1, \beta_1)$: the system is weakly coupled to a reservoir at inverse temperature $\beta_1 > \beta_2$ and quickly relaxes to the initial thermal state A during τ_4. The frequency is again kept constant.

In order to determine the efficiency of the quantum Otto cycle, we need to evaluate work and heat for each of the above steps. During strokes (2) and (4), the frequency is constant, and thus, only heat is exchanged with the reservoirs. On the other hand, during strokes (1) and (3), the system is isolated and work is performed only by modulating the frequency. Since the dynamics is unitary in the latter, the Schrödinger equation for the parametric oscillator can be solved exactly and its mean energy can be obtained analytically using a Gaussian wave function ansatz [29,35,36]. The average quantum energies $\langle H \rangle$ of the oscillator at the four stages of the cycle are

$$\langle H \rangle_A = \frac{\hbar\omega_1}{2} \coth\left(\frac{\beta_1\hbar\omega_1}{2}\right), \tag{1a}$$

$$\langle H \rangle_B = \frac{\hbar\omega_2}{2} Q_1^* \coth\left(\frac{\beta_1\hbar\omega_1}{2}\right), \tag{1b}$$

$$\langle H \rangle_C = \frac{\hbar\omega_2}{2} \coth\left(\frac{\beta_2\hbar\omega_2}{2}\right), \tag{1c}$$

$$\langle H \rangle_D = \frac{\hbar\omega_1}{2} Q_2^* \coth\left(\frac{\beta_2\hbar\omega_2}{2}\right), \tag{1d}$$

where we have introduced the dimensionless adiabaticity parameters Q_1^* and Q_2^* [29]. They are equal to one for adiabatic (slow) processes and increase with the degree of nonadiabaticity. Adiabatic throughout the Letter indicates a process much slower than typical time scales of the system, such as the oscillation period in the trap [37]. The explicit expressions of $Q_{1,2}^*$ for any given modulation ω_t, can be found in Refs. [35,36]. Equations (1a)–(1d) reduce to their classical limits when $\hbar \rightarrow 0$. The mean work, denoted by $\langle W_1 \rangle$, done during the first stroke is

$$\langle W_1 \rangle = \langle H \rangle_B - \langle H \rangle_A = \left(\frac{\hbar\omega_2}{2} Q_1^* - \frac{\hbar\omega_1}{2}\right) \coth\left(\frac{\beta_1\hbar\omega_1}{2}\right), \tag{2}$$

whereas the mean heat $\langle Q_2 \rangle$ exchanged with the hot reservoir during the second stroke reads,

$$\langle Q_2 \rangle = \langle H \rangle_C - \langle H \rangle_B = \frac{\hbar\omega_2}{2}\left[\coth\left(\frac{\beta_2\hbar\omega_2}{2}\right) - Q_1^* \coth\left(\frac{\beta_1\hbar\omega_1}{2}\right)\right]. \tag{3}$$

In a similar way, the average work and heat for the third and fourth stroke are given by,

$$\langle W_3 \rangle = \langle H \rangle_D - \langle H \rangle_C = \left(\frac{\hbar\omega_1}{2} Q_2^* - \frac{\hbar\omega_2}{2}\right) \coth\left(\frac{\beta_2\hbar\omega_2}{2}\right), \tag{4}$$

and

$$\langle Q_4 \rangle = \langle H \rangle_A - \langle H \rangle_D = \frac{\hbar\omega_1}{2}\left[\coth\left(\frac{\beta_1\hbar\omega_1}{2}\right) - Q_2^* \coth\left(\frac{\beta_2\hbar\omega_2}{2}\right)\right]. \tag{5}$$

For a heat engine, heat is absorbed from the hot reservoir, $\langle Q_2 \rangle \geq 0$, and flows into the cold reservoir, $\langle Q_4 \rangle \leq 0$. As a result, the two conditions have to be satisfied:

$$Q_1^* \leq \frac{\coth(\beta_2\hbar\omega_2/2)}{\coth(\beta_1\hbar\omega_1/2)}, \qquad Q_2^* \geq \frac{\coth(\beta_1\hbar\omega_1/2)}{\coth(\beta_2\hbar\omega_2/2)}. \tag{6}$$

The efficiency of this quantum engine, defined as the ratio of the total work per cycle and the heat received from the hot reservoir, then follows as

$$\eta = -\frac{\langle W_1\rangle + \langle W_3\rangle}{\langle Q_2\rangle} = 1 - \frac{\omega_1}{\omega_2}\frac{\coth(\beta_1\hbar\omega_1/2) - Q_2^*\coth(\beta_2\hbar\omega_2/2)}{Q_1^*\coth(\beta_1\hbar\omega_1/2) - \coth(\beta_2\hbar\omega_2/2)}. \quad (7)$$

The above exact expression is valid for arbitrary temperatures and frequency modulations, and allows for a detailed investigation of the performance of the engine.

Efficiency at maximum power.—Two essential characteristics of a heat engine are the power output, $P = -(\langle W_1\rangle + \langle W_3\rangle)/(\tau_1 + \tau_2 + \tau_3 + \tau_4)$, and the efficiency at maximum power [28]. There is generally a trade off between maximum power and maximum efficiency, at which power is zero [38]. Maximum power and the corresponding efficiency can be evaluated analytically for the quantum Otto cycle with the help of Eq. (7). We shall separately consider the case of adiabatic compression or expansion, $Q_{1,2}^* = 1$, and the case of a sudden switch of the frequencies for which $Q_{1,2}^* = (\omega_1^2 + \omega_2^2)/(2\omega_1\omega_2)$. Let us begin with the high-temperature regime $\beta_i\hbar\omega_j \ll 1$, $(i, j = 1, 2)$. The total work produced by the heat engine for a quasistatic frequency modulation is given by

$$\langle W_1\rangle + \langle W_3\rangle = \frac{1}{\beta_1}\left(\frac{\omega_2}{\omega_1} - 1\right) + \frac{1}{\beta_2}\left(\frac{\omega_1}{\omega_2} - 1\right). \quad (8)$$

Assuming that the initial frequency ω_1 (as well as β_1, β_2 and the cycle time) are fixed and by optimizing with respect to the second frequency ω_2, we find that the power is maximum when $\omega_2/\omega_1 = \sqrt{\beta_1/\beta_2}$. As a consequence, the efficiency at maximum power is

$$\eta_{\mathrm{ad}} = 1 - \sqrt{\beta_2/\beta_1}, \quad (9)$$

which corresponds to the Curzon-Ahlborn efficiency [39] (see also Refs. [7,8,25,26]). Conversely, for a sudden frequency switch, the total work is

$$\langle W_1\rangle + \langle W_3\rangle = \frac{1}{2\beta_1}\left[\left(\frac{\omega_2}{\omega_1}\right)^2 - 1\right] + \frac{1}{2\beta_2}\left[\left(\frac{\omega_1}{\omega_2}\right)^2 - 1\right]. \quad (10)$$

By optimizing again with respect to ω_2, we find the power to be maximized when the condition $\omega_2/\omega_1 = \sqrt[4]{\beta_1/\beta_2}$ is satisfied. The corresponding efficiency reads [26],

$$\eta_{\mathrm{ss}} = \frac{1 - \sqrt{\beta_2/\beta_1}}{2 + \sqrt{\beta_2/\beta_1}}. \quad (11)$$

Equations (9) and (11) show that maximum efficiency (of either 1 or 1/2) can be attained when $\beta_1 \to \infty$. Repeating the above optimization analysis in the low-temperature (quantum) regime $\beta_1\hbar\omega_1 \gg 1$, we find for the first time the efficiency at maximum power

$$\eta_{\mathrm{ad}}^q = 1 - \sqrt{\hbar\omega_1\beta_2/2}, \quad (12)$$

for an adiabatic process when $\omega_2 = \sqrt{2\omega_1/\hbar\beta_2}$, and

$$\eta_{\mathrm{ss}}^q = \frac{1 - \sqrt{\hbar\omega_1\beta_2/2}}{2 + \sqrt{\hbar\omega_1\beta_2/2}}, \quad (13)$$

for a sudden frequency switch when $\omega_2 = \sqrt[4]{2\omega_1^3/\hbar\beta_2}$. The above expressions, in which the classical thermal energy $k_B T_1$ is replaced by the ground state energy $\hbar\omega_1/2$ of the oscillator, are the quantum extensions of the Curzon-Ahlborn and Rezek-Kosloff results (9) and (11).

Proposed realization in a Paul trap.—Such a single ion heat engine is composed of one trapped ion in a modified linear Paul trap, as sketched in Fig. 1(c). The trapped ion is initially prepared in a thermal state at low temperature by laser cooling to the Doppler limit in all spatial directions. The engine is driven by alternatingly coupling the ion to two reservoirs that heat and cool the thermal state of the ion in the radial direction through scattering forces. These two baths are realized by differently detuned laser beams on a cycling transition of the trapped ion, irradiated in the radial plane (x, y); the temperature of the reservoirs is controlled by the detuning [40]. In a first step, the coupling to the heat reservoirs is switched on and off externally. The geometry of a trap design with tapered radio-frequency (rf) electrodes leads to a pseudopotential of the form [41],

$$V_p(x, y, z) = \frac{m}{2}\frac{(\omega_{0x}^2 x^2 + \omega_{0y}^2 y^2) r_0^4}{(r_0 + z\tan\theta)^4} + \frac{m}{2}\omega_{0z}^2 z^2, \quad (14)$$

where θ is the angle between the electrodes and the trap axis z, and r_0 the radial distance of the ion to the electrodes, as shown in Fig. 1(c). This potential results in radial trap frequencies that depend on the axial position z, and in an axial force that depends on the radial displacement. The coupling between harmonic axial and radial modes is of the generic form, $H = \sum_{i\in\{x,y,z\}}\hbar\omega_{0i}(a_i^\dagger a_i + 1/2) - C\hat{z}\cdot(\omega_{0x}^2\hat{x}^2 + \omega_{0y}^2\hat{y}^2)$, valid for small z, where $C = 2m\tan\theta/r_0$ denotes the coupling constant between the oscillator modes, and ω_{0i} are the trap frequencies at the center of the trap. A change in energy H of the radial state of the ion, and thus of the width of its spatial distribution, leads to a modification in the axial component of the repelling force which changes the point of equilibrium $z_0(H)$. Heating and cooling the radial state, hence, moves the ion back and forth along the trap axis, as sketched in Fig. 1(b), resulting in the closed Otto cycle shown in Fig. 1(a). This thermally induced axial movement corresponds to the mechanically usable movement of a piston of a classical engine, while the radial mode corresponds to the gas in the cylinder.

The energy gained by running the engine in the radial mode can be stored in the axial mode by exploiting the mode coupling induced by the tapered geometry [see Eq. (14)]. An effective coupling between the modes is avoided through their large frequency difference. However, by

synchronizing the laser cooling or heating (radial) phases to the axial frequency, the work produced can be resonantly converted into an increasing axial oscillation [42]. In principle, the excited axial oscillation is only limited by the trap geometry. Such a power output mechanism is an essential element of a heat engine [7]. The cycle time is given by the axial oscillation period, and is of the order of 10 μs, while the time needed to change the temperature is below 1 μs. In order to reach a steady state, a red-detuned low intensity dissipation laser is applied in the axial direction that damps the coherent movement. The axially stored energy may be transferred to other oscillator systems, e.g., separately trapped ions [43] or nanomechanical oscillators [44], and thus, extracted from the heat engine as usable work. When driven as a heat pump, cooling of such systems should be possible.

The single ion engine offers complete control of all parameters over a wide range. The temperature of the two heat reservoirs, as well as the applied dissipation, can be adjusted by tuning the laser frequencies and intensities. On the other hand, the oscillation amplitude and frequency of the ion can be changed by virtue of the trap parameters. This unique flexibility of the device can be exploited to satisfy the conditions for maximum efficiency at maximum power derived previously.

Monte Carlo simulations.—We have performed extensive semiclassical simulations of the engine by solving the Mathieu equations of motion of the ion, using Monte Carlo and partitioned Runge-Kutta integrators, as described in Ref. [45]. We reach a dynamic confinement of the ion in the trap volume through an oscillating parabolic and tapered saddle potential of the form

$$V_{\mathrm{rf}} \propto \frac{U_0 \sin(\omega_{\mathrm{rf}} t)}{(r_0 + z\tan\theta)^2}(x^2 - y^2), \tag{15}$$

with a trap drive frequency $\omega_{\mathrm{rf}} = 60$ MHz, and the trap geometry described in Fig. 1(c). The thermal state of the ion is generated by a Boltzmann distributed ensemble over several thousand classical trajectories [46]: the initial parameters for each ion are chosen randomly, and the desired thermal probability distribution is reached through the ion-light interaction and the corresponding stochastic spontaneous emission of photons [47]. The switching of the detuned heating and cooling lasers is adjusted to the axial trap frequency ω_z. Each laser is coupled to the ion for 20% of an axial trap period. The ensemble of driven oscillators is thus excited coherently in the axial direction such that heating or cooling takes place at the turning points of the trajectory, independently of the random initial conditions. The (x, p) phase-space distribution, constructed from the simulated trajectories of the ion, is shown in Fig. 3. The radial mode performs the Otto cycle *ABCD*, while the axial (storage) mode oscillates coherently with increasing amplitude α.

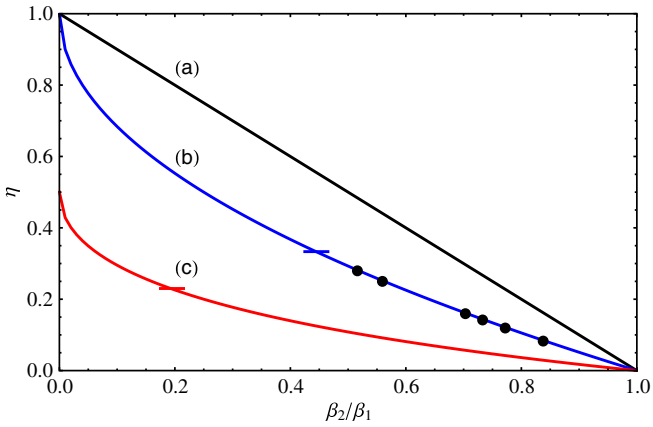

FIG. 2 (color online). Efficiency at maximum power of the Otto engine as a function of the temperature ratio. (a) shows the Carnot efficiency with zero power. (b) corresponds to the theoretical adiabatic process, Eq. (9), while (c) corresponds to the sudden frequency switch, Eq. (11). The black points denote the results of the numerical simulations with realistic trap parameters, and demonstrate that the engine can run at maximum efficiency at maximum power. The horizontal bars indicate estimated upper bounds at $\omega_2 = 1.5\omega_1$.

Radial temperatures in the range of 20 to 200 mK were achieved, corresponding to $0.1 < \beta_2/\beta_1 < 1$ and respective radial phonon numbers of about 400 and 4000 [48]. In the simulations the temperature is determined via the mean energy, $\langle H \rangle = k_B T$; in an experiment, it can be determined via the method presented in Ref. [49]. For a realistic maximal axial amplitude of about 1 mm, the relative variation of the radial frequency at 6.0 MHz is about 50%. By properly adjusting the parameters to satisfy the optimality condition in the quasiadiabatic regime, our simulations show that this Otto engine has the ability to run at maximum efficiency at maximum power in the interval $0.5 < \beta_2/\beta_1 < 1$ (see Fig. 2). The efficiency is determined via Eq. (7) from simulated cycles as shown in Fig. 1(a) by evaluating the energy differences $\langle W_1 \rangle$, $\langle W_3 \rangle$, and $\langle Q_2 \rangle$ between the points

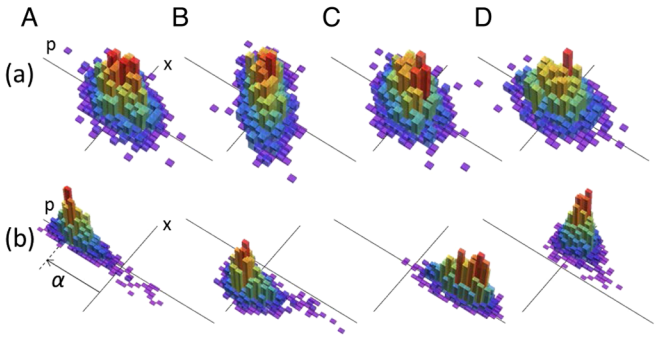

FIG. 3 (color online). Phase-space distribution of the motional state of the ion during an engine cycle: (a) The radial modes perform the full Otto cycle *ABCD*. (b) Coherent oscillations (with typical displacement of $\alpha = 10^3$ wave packets) of the axial mode used to store the produced work.

ABCD. The power is obtained by dividing the total work by the (constant) cycle time. The maximum efficiency is about 30% and significantly larger than those obtained to date [18,19]. The power is of the order of $P \simeq 10^{-20}$ J/s. The adiabaticity parameter $Q^*_{1(2)}$, given by the ratio of the action $\langle H \rangle / \omega$ [37] at points B and A (D and C), see Eq. (1), is about 1.02. The case of a sudden switch can be realized by exchanging the values of radial and axial frequencies. Contrary to the adiabatic limit, the optimality condition can be achieved down to $\beta_2/\beta_1 \simeq 0.2$. However, the maximum efficiency reduces to 23%.

While so far the laser reservoirs have, for simplicity, been switched on and off externally, another feature of this Otto engine is the ability to operate in a completely self-driven manner. To this end, the foci of the heating and cooling lasers can be separated spatially on the trap axis by, e.g., 200 μm, so that the ion is coupled to the heat baths at the turning points of its axial trajectory. No active switching is required and the axial motion of the ion is self-amplifying. The ion needs to be driven only in the initial phase of the axial motion to reach a threshold amplitude. We note that at a radial frequency of 6.0 MHz, the thermal energy of the oscillator, Eq. (1a), starts to deviate appreciably from its classical value below 200 μK, which could be reached with ^{40}Ca-ions, if we assume a two-level approximation and the Doppler cooling limit $T_D = \hbar\Gamma/(2k_B)$, where Γ denotes the linewidth of the dipole transition. A single ion engine has thus the potential to enter the quantum regime and become a tool to study effects of quantum coherence and correlations on the efficiency [9,13]. Application of optimal control techniques [50] would further allow for nonclassical bath engineering. The investigation of heating and cooling on the simple and fundamental single ion mode interactions may serve for prototyping heaters or coolers also in systems, which share similar properties. For the specific example of micromechanical oscillators, mode coupling has been described and realized in several experiments [33,34].

Conclusion.—We have put forward a realistic proposal for a tunable nanoengine based on a single ion in a tapered linear Paul trap coupled to engineered laser reservoirs. The operation in the Otto cycle would result in coherent ion motion. Combining analytical and numerical analysis, we have studied the performance of the engine and showed that it can run at maximum power in a wide range of temperatures. We have, moreover, introduced a generic power output mechanism which is crucial for the technological development of nanoengines.

We thank U. Poschinger for carefully reading the manuscript. This work was supported by the Emmy Noether Program of the DFG (Contract No. LU1382/1-1), the cluster of excellence Nanosystems Initiative Munich (NIM), the Alexander-von-Humboldt Foundation, the Volkswagen-Stiftung, the DFG-Forschergruppe (FOR 1493), and the EU project DIAMANT (FP7-ICT).

[1] G. Cerefolini, *Nanoscale Devices* (Springer, Berlin, 2009).
[2] Y. A. Cengel and M. A. Boles, *Thermodynamics. An Engineering Approach* (McGraw-Hill, New York, 2001).
[3] E. R. Kay, D. A. Leigh, and F. Zerbetto, Angew. Chem., Int. Ed. Engl. **46**, 72 (2007).
[4] P. Hänggi and F. Marchesoni, Rev. Mod. Phys. **81**, 387 (2009).
[5] H. E. D. Scovil and E. O. Schulz-DuBois, Phys. Rev. Lett. **2**, 262 (1959).
[6] R. Alicki, J. Phys. A **12**, L103 (1979).
[7] R. Kosloff, J. Chem. Phys. **80**, 1625 (1984).
[8] E. Geva and R. Kosloff, J. Chem. Phys. **96**, 3054 (1992); **97**, 4398 (1992).
[9] M. O. Scully, Phys. Rev. Lett. **88**, 050602 (2002).
[10] T. E. Humphrey, R. Newbury, R. P. Taylor, and H. Linke, Phys. Rev. Lett. **89**, 116801 (2002).
[11] M. O. Scully, M. S. Zubairy, G. S. Agarwal, and H. Walther, Science **299**, 862 (2003).
[12] T. D. Kieu, Phys. Rev. Lett. **93**, 140403 (2004).
[13] R. Dillenschneider and E. Lutz, Europhys. Lett. **88**, 50 003 (2009).
[14] J. Gemmer, M. Michel, and G. Mahler, *Quantum Thermodynamics* (Springer, Berlin, 2009).
[15] T. Hugel, N. B. Holland, A. Cattani, L. Moroder, M. Seitz, and H. E. Gaub, Science **296**, 1103 (2002).
[16] S. A. Jacobson and A. H. Epstein, in *Proceedings of the International Symposium on Micro-Mechanical Engineering, Tsuchiura and Tsukuba, Japan, 2003*, pp. 513–520.
[17] S. Whalen, M. Thompson, D. Bahr, C. Richards, and R. Richards, Sens. Actuators **104**, 290 (2003).
[18] P. G. Steeneken, K. Le Phan, M. J. Goossens, G. E. J. Koops, G. J. A. M. Brom, C. van der Avoort, and J. T. M. van Beek, Nat. Phys. **7**, 354 (2011).
[19] V. Blickle and C. Bechinger, Nat. Phys. **8**, 143 (2012).
[20] D. Leibfried, R. Blatt, C. Monroe, and D. Wineland, Rev. Mod. Phys. **75**, 281 (2003).
[21] J. F. Poyatos, J. I. Cirac, and P. Zoller, Phys. Rev. Lett. **77**, 4728 (1996).
[22] R. Blatt and D. Wineland, Nature (London) **453**, 1008 (2008).
[23] T. Monz, P. Schindler, J. Barreiro, M. Chwalla, D. Nigg, W. Coish, M. Harlander, W. Hänsel, M. Hennrich, and R. Blatt, Phys. Rev. Lett. **106**, 130506 (2011).
[24] G. Huber, F. Schmidt-Kaler, S. Deffner, and E. Lutz, Phys. Rev. Lett. **101**, 070403 (2008).
[25] B. Lin and J. Chen, Phys. Rev. E **67**, 046105 (2003).
[26] Y. Rezek and R. Kosloff, New J. Phys. **8**, 83 (2006).
[27] H. T. Quan, Y. X. Liu, C. P. Sun, and F. Nori, Phys. Rev. E **76**, 031105 (2007).
[28] B. Andresen, P. Salamon, and R. S. Berry, Phys. Today **37**, No. 9, 62 (1984).
[29] K. Husimi, Prog. Theor. Phys. **9**, 381 (1953).
[30] F. Tonner and G. Mahler, Phys. Rev. E **72**, 066118 (2005).
[31] A. D. O'Connell *et al.*, Nature (London) **464**, 697 (2010).
[32] Q. Lin, J. Rosenberg, D. Chang, R. Camacho, M. Eichenfield, K. J. Vahala, and O. Painter, Nature Photon. **4**, 236 (2010).
[33] R. B. Karabalin, M. C. Cross, and M. L. Roukes, Phys. Rev. B **79**, 165309 (2009).

[34] T. Faust, J. Rieger, M. J. Seitner, P. Krenn, J. P. Kotthaus, and E. M. Weig, Phys. Rev. Lett. **109**, 037205 (2012).
[35] S. Deffner and E. Lutz, Phys. Rev. E **77**, 021128 (2008).
[36] S. Deffner, O. Abah, and E. Lutz, Chem. Phys. **375**, 200 (2010).
[37] L. D. Landau and E. M. Lifshitz, *Mechanics* (Pergamon, Oxford, 1960), Sect. 49.
[38] H. S. Leff, Am. J. Phys. **55**, 602 (1987).
[39] F. L. Curzon and B. Ahlborn, Am. J. Phys. **43**, 22 (1975).
[40] J. I. Cirac, R. Blatt, P. Zoller, and W. D. Phillips, Phys. Rev. A **46**, 2668 (1992); J. I. Cirac, M. Lewenstein, and P. Zoller, Phys. Rev. Lett. **72**, 2977 (1994).
[41] B. B. Blinov, D. Leibfried, C. Monroe, and D. J. Wineland, Quantum Inf. Process. **3**, 45 (2004).
[42] Since laser and axial directions are perpendicular, there is no interaction between laser reservoirs and axial mode.
[43] M. Harlander, R. Lechner, M. Brownnutt, R. Blatt, and W. Hänsel, Nature (London) **471**, 200 (2011).
[44] L. Tian and P. Zoller, Phys. Rev. Lett. **93**, 266403 (2004).
[45] K. Singer, U. Poschinger, M. Murphy, P. Ivanov, F. Ziesel, T. Calarco, and F. Schmidt-Kaler, Rev. Mod. Phys. **82**, 2609 (2010).
[46] R. Casdorff and R. Blatt, Appl. Phys. B **45**, 175 (1988).
[47] M. Srednicki, Phys. Rev. E **50**, 888 (1994).
[48] Heating through electrode noise would add 4.10^{-5} quanta per cycle, assuming a heating rate of 1 quantum per 250 ms. It is, thus, negligible; see C. Roos, T. Zeiger, H. Rohde, H. C. Ngerl, J. Eschner, D. Leibfried, F. Schmidt-Kaler, and R. Blatt, Phys. Rev. Lett. **83**, 4713 (1999).
[49] J. H. Wesenberg *et al.*, Phys. Rev. A **76**, 053416 (2007).
[50] M. Schmidt, A. Negretti, J. Anderhold, T. Calarco, and J. T. Stockburger, Phys. Rev. Lett. **107**, 130404 (2011).